Understanding the Hydrogen Bond in Terms of the Location of the Bond Critical Point and the Geometry of the Lone Pairs

Anupama Ranganathan, G. U. Kulkarni, and C. N. R. Rao*

Chemistry and Physics of Materials Unit, Jawaharlal Nehru Centre for Advanced Scientific Research, Jakkur P.O., Bangalore 560 064, India

Received: April 17, 2003

The experimental charge density method has been employed to provide a more detailed description of the hydrogen bond in terms of the location of the bond critical point and the geometry of the lone pair of electrons. On the basis of a study of 7 different O−H···O hydrogen-bonded systems with 19 hydrogen bonds covering a wide range of hydrogen bond distances and angles, it has been possible to arrive at a generalization of the topological descriptors. In all of the hydrogen bonds studied, the electron density at the bond critical point (BCP) and its Laplacian fall in the range of 0.03−0.39 eÅ^{-3} and 0.7−6.0 eÅ^{-5}, respectively. The bond paths deviate, in some instances widely, from the H···O bond axis, and the resulting d_{CP} values (vertical displacement of the bond critical point from the internuclear line) range from 0.036 to 0.418 Å. The origin of such high d_{CP} values has been related to the constellation of the various interaction centers—the lone pairs and the atom cores of the donor and the acceptor oxygens and the hydrogen atom. This study provides a useful classification of the hydrogen bonds in terms of a new interaction line, L_{i-j}, connecting the various centers i and j. A nearness parameter, d_L, that represents the perpendicular distance of the critical point from the interaction line, L_{i-j}, justifies the classification. The d_L values are found to be much smaller than the corresponding d_{CP} values.

Introduction

The experimental charge density method based on X-ray crystallography has been employed successfully during the last two decades to understand the bonding and properties of molecular systems.[1] For instance, the biomolecular functionality of amino acids and oligopeptides has been extensively studied by analyzing their electrostatic potentials.[2] In-crystal molecular properties related to nonlinear optical activity[3,4] and pyroelectricity[5] have been evaluated by employing experimental charge density. The extent of conjugation in ring systems such as benzene,[6] imidazole, triazole, pyrimidine derivatives,[7] and annulene[8] as well as in the cubane cage[9] has been examined. An analysis of the squarate and croconate dianions in comparison to many other aromatic and nonaromatic cyclic systems was reported recently.[10] There have been several experimental charge density studies on hydrogen-bonded systems, most pertaining to O−H···O,[11] N−H···O,[12] and N−H···N[13] bonds, whereas weak C−H···O,[14] N−H···π,[15] and C−H···π[16] interactions have been explored only recently. There are also electron density investigations on crystals that host combinations of strong and weak hydrogen bonds.[4c,17] In general, the total density at the bond critical points of the hydrogen bonds in all such systems is generally in the range of 0.01−0.6 eÅ^{-3}, and the Laplacians are positive and fall in the range of 0.3−6.0 eÅ^{-5}.

Systematic correlations between the electron density parameters and the hydrogen bond geometry have been reported by a few workers.[18] Thus, Lecomte and co-workers[19] related the structural parameters and the topological properties at the bond critical points such as the electron density, ρ_{BCP}, the Laplacian of the electron density, $\nabla^2\rho_{BCP}$, and the positive curvature of ρ_{BCP} along the internuclear axis, λ_3. These workers have shown that the positive curvature of the electron density (λ_3) relates well to the hydrogen bond distance. Furthermore, for closed-shell interactions, the kinetic energy density, $G(r_{CP})$, and the potential energy density, $V(r_{CP})$, at the critical point depend exponentially on the H···O distance.[20] These workers have also described relationships between the kinetic and potential energy densities and the curvatures of the electron density at the critical point (CP).[21] Woźniak et al.[22] have analyzed the charge density distribution in the N−H···O and C−H···O bonds of dipicrylamine and have shown a linear relationship between the charge density at the CPs and the N···O contact distance. A charge density study of symmetric and asymmetric O−H···O bonds in dimethylammonium hydrobis(squarate) by Lin et al.[23] has revealed that the electron density of the carbonyl oxygen lone pairs has a mixed nature between the sp^3 and sp^2 hybrids. There are also theoretical efforts to relate distances and the electron density parameters at the bond critical point.[24]

We have been interested in understanding the topological properties of the experimental charge densities in hydrogen bonds, especially with respect to the location of the critical points and bond paths as well as the relation between the critical points and the geometry of the lone pairs on the donor and the acceptor atoms. In this article, we report the results of a careful analysis of the experimental charge densities of O−H···O bonds of different geometries present in the following hydrogen bond systems: a piperazine−oxalate complex (**I**), the α form of ethoxy cinnamic acid (**II**), adipic acid (**III**), disodium salts of croconic (**IV**), and squaric (**V**) acids. These systems possess linear, bifurcated, and trifurcated hydrogen bonds with a range of angles and H···O distances. Besides enabling a complete charge density description of the hydrogen bond, the present study provides new and important insights with respect to the

* To whom correspondence should be addressed. E-mail: cnrrao@jncasr.ac.in.

10.1021/jp030465m CCC: $25.00
Published on Web 07/15/2003

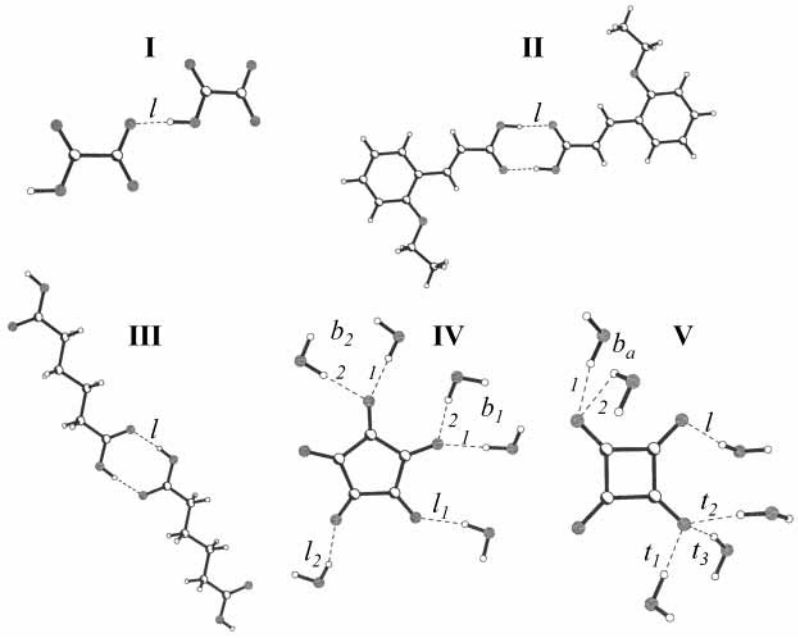

Figure 1. Diagrammatic representation of the hydrogen bonds chosen for the study. **I**, the oxalate ion of the piperazine oxalate complex; **II**, α-ethoxy cinnamic acid; **III**, adipic acid; **IV**, the croconate dianion; **V**, the squarate dianion.

TABLE 1: Refinement Parameters for Compounds I−V

	I	II	III	IV	V
Crystallographic information may be obtained from the deposition numbers in the Cambridge Crystallographic Data Centre (CCDC).	CCDC 203885	CCDC 205456	ADIPAC05	CCDC 171699	CCDC 171698
after multipole refinement weighting scheme	0.051, 0.095	0.070, 0.123	0.063, 0.113	0.057, 0.114	0.047, 0.094
$R\{F\}$	0.0310	0.0426	0.0493	0.0392	0.0366
$R\{F^2\}$	0.0501	0.0467	0.0868	0.064	0.07
S	1.024	0.9808	0.9685	1.196	1.0496
no. of variables	253	272	100	263	245
N_{ref}/N_v	20.5099	14.3382	24.5100	23.0342	25.8122

location of the critical point and its relation to the lone pairs involved in the formation of the hydrogen bonds and is therefore useful for a better understanding of the hydrogen bond, in general. Being entirely based on an experimental charge density analysis, the results reported here are of significance.

Experimental Section

X-ray diffraction data were collected at low temperature (130 K) using a Siemens three-circle diffractometer attached to a CCD area detector and a graphite monochromator for Mo Kα radiation. The **II**[25] and **V**[10] systems crystallize in a triclinic space group (*P*-1); therefore, to increase the redundancy in the data, full-sphere data were collected in two shells with different 2θ settings of the detector (28 and 70°). However, hemisphere data were found to be sufficient for **I**,[26] **III**,[27] and **IV**[10] because they belonged to monoclinic space groups. Data reduction was performed using the SAINT program (Siemens, U.S.A., 1995). Data with $\sin\theta/\lambda$ up to ~1.1 Å^{-1} were thus obtained. The phase problem was solved by direct methods, and the non-hydrogen atoms were refined anisotropically by means of the full-matrix least-squares procedure using the SHELXTL program (Siemens, U.S.A., 1995). The H-atom positions were found using the difference Fourier method and were adjusted to average neutron values[28] as a routine pretreatment to the multipole refinement.

TABLE 2: Bond Distances and Angles of the Various Hydrogen Bonds

system	type of H bond	O−H (Å)	H···O (Å)	O−H···O (°)
I	linear (l)	1.015(10)	1.532(9)	174.1(16)
II	linear (l)	0.97(3)	1.68(2)	172.1(6)
III	linear (l)	0.958(19)	1.72(2)	173(3)
IV	linear (l_1)	0.960(3)	1.841(5)	166.9(17)
	linear (l_2)	0.960(7)	1.998(7)	164.5(15)
	bifurcated (b_{11})	0.959(7)	1.829(7)	171.9(17)
	bifurcated (b_{12})	0.961(8)	1.797(8)	171.1(14)
	bifurcated (b_{21})	0.961(13)	1.889(14)	176.2(16)
	bifurcated (b_{22})	0.961(8)	1.817(6)	170.9(17)
V	linear (l)	0.959(9)	1.912(8)	166.4(12)
	bifurcated (b_{a1})	0.961(18)	1.871(19)	163.8(19)
	bifurcated (b_{a2})	0.955(15)	2.495(17)	131.0(13)
	trifurcated (t_1)	0.960(13)	1.714(13)	169.6(12)
	trifurcated (t_2)	0.961(12)	1.873(12)	172.5(10)
	trifurcated (t_3)	0.960(9)	1.938(10)	163.9(14)

All of the hydrogen atoms were held constant throughout the refinement along with their isotropic temperature factors. Hydrogen bonds were analyzed using the PLATON package.[29] The molecular diagrams of the chosen set depicting the various hydrogen bond patterns are shown in Figure 1. Crystallographic information may be obtained using CCDC access codes listed in Table 1. The geometrical parameters of the hydrogen-bonded systems are listed in Table 2.

Charge Density Analysis

The charge density was modeled using the standard approach, the details of which may be found elsewhere.[1b] In brief, the analysis was carried out on the basis of a multipole expansion of the electron density centered at the nucleus of the atom. Accordingly, the aspherical atomic density can be described in terms of spherical harmonics,

$$\rho_{atom}(r) = \rho_{core}(r) + \rho_{valence}(r) + \rho_{def}(r)$$

Thus, for each atom,

$$\rho_{atom}(r) = \rho_{core}(r) + P_V\kappa^3\,\rho_{valence}(\kappa r) + \sum_{l=0}\kappa'^3\,R_l(\kappa'\xi r)\sum_{m=0}\sum_{p=\pm l}P_{lmp}\,Y_{lmp}(\theta,\varphi)$$

with the origin at the atomic nucleus. The population coefficients, P_{lmp}, were refined along with the κ and κ' parameters that control the radial dependence of the valence shell density. The XDLSM routine of the XD package was used for this purpose.[30] The atomic coordinates and the thermal parameters obtained from a high-order refinement ($\sin\theta/\lambda > 0.6$ Å^{-1}) were used as input to XD refinement. The Hirshfeld criterion was satisfied in all cases.[31]

The deformation density was obtained by subtracting the spherical atomic densities (the promolecular density) from the total charge density ($\delta\rho(r) = \rho^{total}(r) - \rho^{pro}(r)$).[32,33] The important bond parameters are the total density at the bond critical point (ρ_{BCP}) and its Laplacian ($\nabla^2\rho_{BCP}$), which is the arithmetic sum of the three eigenvalues ($\lambda_1 + \lambda_2 + \lambda_3$) along the principal axes. Another important property of the bonded interaction is the bond path (BP), which is a topological expression for the line of maximum charge density linking two nuclei via the bond critical point (BCP).[34] The geometrical parameter, d_{CP}, is the perpendicular distance of the BCP from the internuclear axis. It gives a measure of the strain or the bent nature of the bonds. The nature of the nonbonded density can be analyzed by a CP search in the deformation density[35] or the Laplacian of the total density where the lone-pair electrons occur as (3, −3) CPs.[36] The XDPROP routine was used for all of the above purposes.

Results and Discussion

Before discussing the results of the critical point analysis, a brief geometrical description of the hydrogen-bonded systems is provided. As shown in Figure 1, piperazine−oxalate (**I**) forms a linear O−H···O bond (designated as *l*) with an H···O distance of 1.532(9) Å and an angle of 174.1(16)°. α-Ethoxy cinnamic acid (**II**) and adipic acid (**III**) form centrosymmetric dimers (*l*) of comparable geometries (Figure 1 and Table 2). The croconate ion (**IV**), in the monoclinic form of the disodium salt, forms four O−H···O bonds with the surrounding water molecules grouped into two bifurcated systems (designated as *b* in Figure 1). In each case, an acceptor oxygen atom makes contacts with two hydrogen atoms from different water donor groups.[37] The other hydrogen on water is involved in a bifurcated bond originating from a neighboring croconate ion (not shown in the Figure). Thus, b_{11} and b_{21} bonds share a common donor, and so does the b_{12} and b_{22} pair. As shown in Table 2, the H···O bond lengths are spread between 1.8 and 1.9 Å, with O−H···O angles between 170 and 176°. The bifurcation angles (angle between the two O−H···O bonds) are 88.6 and 85.1° for b_1 and b_2, respectively. The croconate ion also forms two linear bonds (l_1 and l_2) with the water molecules (Figure 1 and Table 2). The water molecule engaged in l_1 forms an l_2 hydrogen bond with a neighboring croconate ion. This results in a network of croconate ions linked by bifurcated and linear bonds from the surrounding water molecules. A unique feature of the squarate ion (**V**) is the presence of the trifurcated hydrogen bond (designated as *t*) in the squarate ion, where the acceptor oxygen atom makes contact with three water donor groups. The squarate ion also exhibits a bifurcated bond, b_a, that is highly asymmetrical (Table 2). Thus, the chosen set of hydrogen bonds is truly representative of the broad range of H···O distances (1.53 to 2.50 Å) and angles (176 to 130°). The O−H distance is close to 0.96 Å in all cases except two (**I** and **II**), where the bonds are slightly elongated and the corresponding H···O distances are shorter (Table 2).

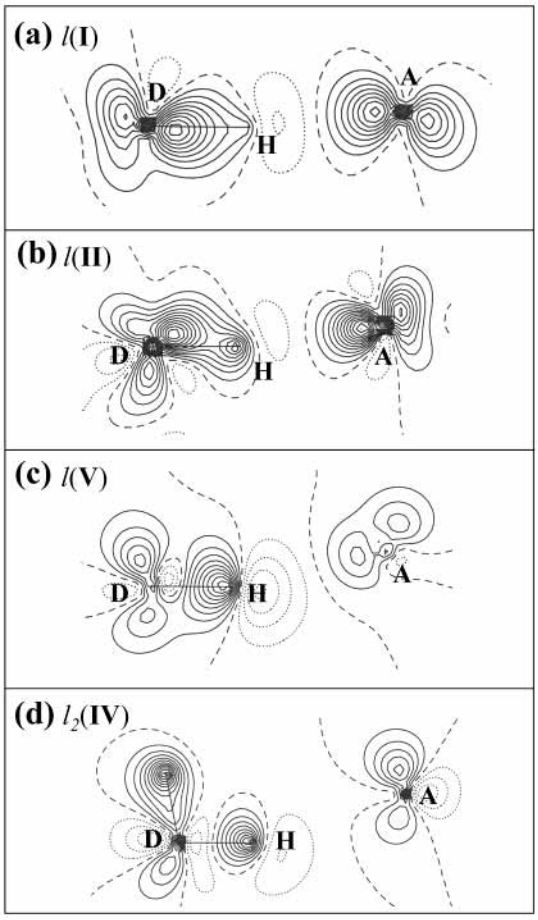

Figure 2. Static deformation density plots (at contour intervals of 0.1 eÅ^{-3}) in the hydrogen bond plane. D, H, and A stand for the donor, hydrogen, and acceptor atoms. (a) *l*(**I**), (b) *l*(**II**), (c) *l*(**V**), (d) l_2(**IV**).

In Figure 2, the static deformation density maps in the hydrogen bond (O−H···O) plane are shown for four examples. The maps reveal chemically significant features such as bonding regions and lone-pair (nonbonding) regions. Concentric contours between the atom cores typify the bonding regions, and localized lobes attached to the oxygen core represent the lone pairs. From Figure 2a−d, we see that there is an accumulation of charge density in the O−H regions, which is typical of a shared interaction. However, there is a depletion of the charge density in the H···O region. This is taken to represent a closed-shell interaction between the hydrogen and the acceptor. The distribution of electron density is so varied among the different bonds that it brings out the diverse nature of the hydrogen bond. The positions of the lone-pair CPs relative to the donor and the acceptor cores are shown in Figure 3. The values of the total

TABLE 3: Geometries of the Lone Pairs on the Donor and Acceptor Atoms of the O−H···O Bonds

system	type of H bond	d_{D-l} (Å)		d_{A-l} (Å)		φ_D, φ_A (°)		ω_D, ω_A (°)	
I	linear (l)	0.261	0.332	0.265	0.263	94.7	145.6	134.3	135.1
II	linear (l)	0.249	0.256	0.254	0.240	140.6	134.7	49.3	48.2
III	linear (l)	0.262	0.238	0.256	0.260	171.3	165.5	123.6	38.5
IV	linear (l_1)	0.268	0.290	0.279	0.280	159.8	159.2	55.8	176.3
	linear (l_2)	0.268	0.290	0.290	0.295	159.8	154.2	107.6	168.8
	bifurcated (b_{11})	0.284	0.287	0.279	0.280	148.5	159.1	75.1	144.0
	bifurcated (b_{12})	0.287	0.276	0.279	0.280	162.4	159.1	124.1	70.2
	bifurcated (b_{21})	0.284	0.287	0.280	0.280	148.5	159.1	153.5	104.0
	bifurcated (b_{22})	0.287	0.276	0.280	0.280	162.4	159.1	70.2	80.4
V	linear (l)	0.344	0.513	0.336	0.333	116.0	133.3	110.4	162.9
	bifurcated (b_{a1})	0.339	0.330	0.352	0.348	146.7	131.4	40.9	28.7
	bifurcated (b_{a2})	0.323	0.321	0.352	0.348	142.1	131.4	87.0	52.9
	trifurcated (t_1)	0.323	0.321	0.337	0.333	142.1	133.2	55.9	142.3
	trifurcated (t_2)	0.344	0.513	0.337	0.333	116.0	133.2	95.7	127.3
	trifurcated (t_3)	0.339	0.330	0.337	0.333	146.7	133.2	80.2	82.1

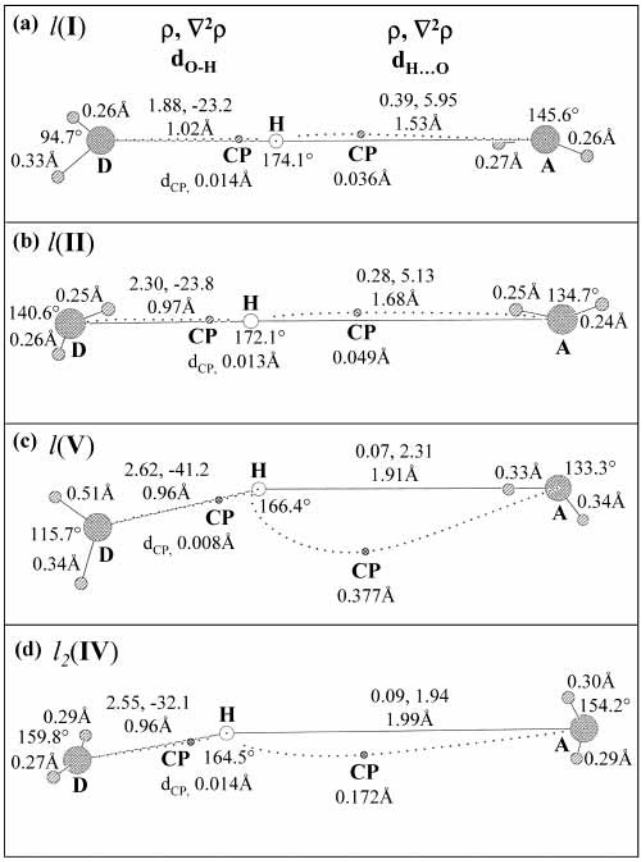

Figure 3. Charge density parameters of the O−H···O bonds: large hatched circles, donor (D) and acceptor (A) cores; open circles, hydrogen (H); small hatched circles, lone-pair electrons; small filled circles, D−H and H···A critical points (CP). The values of ρ and $\nabla^2\rho$ are given in eÅ^{-3} and eÅ^{-5}, respectively. The O−H and H···O distances (d_{O-H} and $d_{H\cdots O}$) are shown above the bonds. The value of d_{CP} is shown below the CP symbol. The distance of the lone-pair lobe to the donor or the acceptor atom core is indicated adjacent to the lone-pair circles. Values of φ_D and φ_A (see text) are shown close to the donor and acceptor atoms.

density at the lone-pair CPs are around 7 eÅ^{-3} with Laplacians of ca. −115 eÅ^{-5}, in agreement with those reported for oxygen lone pairs.[1e] Table 3 lists the geometrical parameters of the (3, −3) lone-pair CPs for all of the hydrogen bonds obtained using the XDPROP routine. The distance from the eye of the lone-pair lobe (the CP) to the atomic (donor or acceptor) core is around 0.3 Å, except in a few cases where the distance extends to 0.5 Å. The distances agree well with the reported values in the literature.[11b,h] The angles between the lone pairs at the atomic core (φ_D and φ_A) are usually in the range of 130 to 160°. Such high angles can be attributed to the lone pair−lone pair repulsion. We observe smaller angles (at 94 and 116°) in a few cases, especially with respect to the donors. We also estimated the angle subtended by the plane formed by the core of the donor and its lone pairs with the hydrogen bond plane, ω_D, and the corresponding angle at the acceptor site, ω_A. The values are similar (134.3 and 135.1°) in the case of the linear hydrogen bond l(**I**). This is also the case for the l(**II**) and the t_3(**V**) bonds. For the rest of the hydrogen bonds, the two angles are different (Table 3).

The linear bond l(**I**) exhibits electron densities of 1.88(6) and 0.39(4) eÅ^{-3} at the O−H and H···O BCPs, respectively (Figure 3a and Table 4). The corresponding Laplacian values are −23.2(4) and 5.95(8) eÅ^{-5}, respectively. The small and positive Laplacian of the H···O bond is typical of a closed-shell interaction, and a highly negative Laplacian of the O−H bond is due to the shared interaction. The d_{CP} value for the H···O bond is slightly higher (0.036 Å) than that for the O−H bond (0.014 Å). Accordingly, the bond path (BP) in the H···O region is displaced slightly from the line joining the two atoms. This is also the case with the linear bond l(**II**) (Figure 3b). The l(**V**) bond (Figure 3c) carries much less density (0.07(3) eÅ^{-3}) and Laplacian of 2.31(1) eÅ^{-5}, and the BP is noticeably curved with a d_{CP} value of 0.377 Å. This is indeed surprising because its geometry is not so unfavorable (H···O, 1.912(8)Å, 166.4(12)°). Similar values have been obtained for the l_2(**IV**) bond (Figure 3d). As expected, hydrogen bonds with relatively short H···O distances and angles close to 180° generally exhibit higher densities and Laplacians at the BCPs.[38] The BPs are less curved in such cases and are associated with small d_{CP} values. From Table 4, we notice that the d_{CP} values of the H···O bonds are often 1 order higher than the corresponding d_{CP} values of the O−H bonds. On the basis of a study of a variety of hydrogen bonds, Lecomte and co-workers have reported H···O d_{CP} values of up to 0.12 Å for H···O distances ranging from 1.22 to 1.97 Å.[19]

The d_{CP} values of the H···O bonds are indeed unusual and do not occur in normal shared interactions. If a covalent bond has a slightly higher d_{CP} value, say ∼0.05 Å, then the bond is considered to be strained. One comes across such situations in strained ring systems. For instance, the mean d_{CP} value of the C−C bonds in the squarate ring is 0.058 Å,[10] which is comparable to that in the cyclobutyl ring of α-truxillic acid (0.046 Å).[19a] A highly strained cyclopropyl ring exhibits a value of 0.06 Å.[39] The cage bonds in a 1,2-difluorinated cubane derivative have an average d_{CP} value of 0.14 Å.[9] Because the hydrogen bond interaction is mainly electrostatic (closed shell),

TABLE 4: Charge Density Parameters for the O−H and H···O Bonds of the Chosen Hydrogen-Bonded Systems[a]

		O−H			H···O		
system	type of H bond	ρ (eÅ^{-3})	$\nabla^2\rho$ (eÅ^{-5})	$d_{CP} \times 10^2$ (Å)	ρ (eÅ^{-3})	$\nabla^2\rho$ (eÅ^{-5})	$d_{CP} \times 10^2$ (Å)
I	linear (l)	1.88(6)	−23.2(4)	1.4	0.39(4)	5.95(8)	3.6
II	linear (l)	2.3(1)	−23.8(8)	1.3	0.28(7)	5.13(8)	4.9
III	linear (l)	2.6(1)	−54.0(9)	0.6	0.21(7)	6.17(9)	12.8
IV	linear (l_1)	2.77(9)	−29.5(7)	1.5	0.21(3)	3.02(1)	6.0
	linear (l_2)	2.55(10)	−32.1(6)	1.4	0.09(3)	1.94(1)	17.2
	bifurcated (b_{11})	2.70(9)	−25.5(6)	1.5	0.21(3)	3.00(1)	8.4
	bifurcated (b_{12})	2.92(9)	−42.2(7)	0.7	0.18(3)	2.97(1)	5.4
	bifurcated (b_{21})	2.90(9)	−30.2(5)	0.9	0.09(3)	2.52(1)	18.3
	bifurcated (b_{22})	2.93(9)	−26.4(6)	0.9	0.20(3)	3.32(1)	4.3
V	linear (l)	2.62(9)	−41.2(5)	0.8	0.07(3)	2.31(1)	37.7
	bifurcated (b_{a1})	2.64(8)	−39.6(5)	2.4	0.14(3)	2.95(1)	24.0
	bifurcated (b_{a2})	2.65(8)	−32.7(4)	1.8	0.03(1)	0.647(3)	41.8
	trifurcated (t_1)	2.40(7)	−33.5(4)	2.1	0.23(3)	4.44(3)	14.6
	trifurcated (t_2)	2.35(7)	−36.0(5)	1.3	0.11(3)	3.56(3)	10.1
	trifurcated (t_3)	2.36(7)	−23.3(4)	1.5	0.14(3)	2.75(1)	9.7

[a] Here, ρ (eÅ^{-3}) is the electron density at the bond critical point, $\nabla^2\rho$ (eÅ^{-5}) is the Laplacian of the electron density at the bond critical point, and d_{CP} is the perpendicular distance of the critical point from the bond axis.

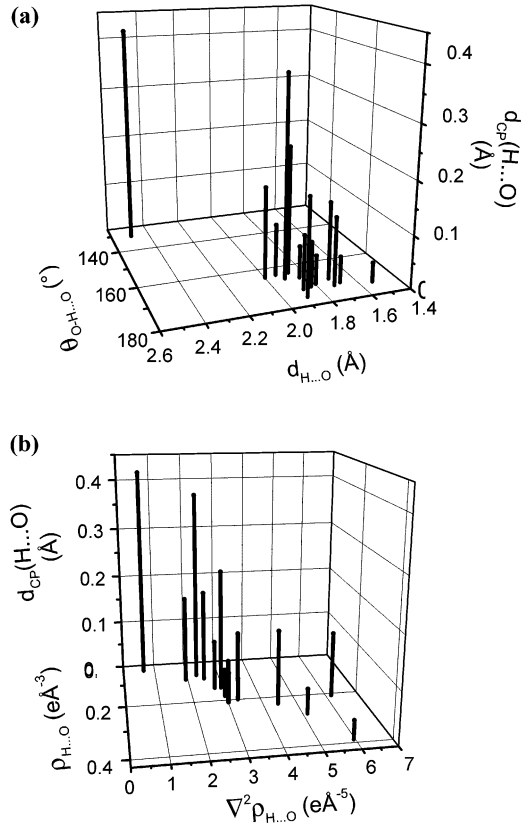

Figure 4. Histograms depicting d_{CP} against (top) the O−H···O angle and the $d_{H\cdots O}$ (bottom) total density and its Laplacian at the H···O CP.

a simple "bent-bond" description would not be adequate, especially in situations where the d_{CP} values are high. We have therefore attempted to relate d_{CP} values of the H···O bonds to the H···O distance, O−H···O angle, ρ_{BCP}, and $\nabla^2\rho_{BCP}$ (Figure 4). The plot in Figure 4a shows how short H···O distances and angles close to 180° are generally associated with small d_{CP} values. The l bond in **III** and l_2 and b_{21} bonds in **IV** seem to be exceptions. The data points in ρ_{BCP} and $\nabla^2\rho_{BCP}$ are somewhat spread (Figure 4b), but it appears that small d_{CP} values accompany high values of the density and the Laplacian.

We have found it instructive to examine the bond paths of the H···O bonds. The BP essentially lies in a plane that is different from the O−H···O plane. Small deviations of the BP from its mean plane are usually observed close to the atom cores. We have presented the BPs of the various H···O bonds in a single normalized plot in Figure 5. Each BP starts at the hydrogen core with a characteristic takeoff, bends inwardly after covering nearly one-third of the H···O distance, and then approaches the acceptor core with no appreciable curvature. The bond CP is located close to where the BP bends, giving rise to a high d_{CP} value (Table 4). We find that the takeoff angle is related to the d_{CP} value as shown in the inset of Figure 5. The Figure reveals that high values of d_{CP} are associated with unusual BP takeoff angles. An exact description of the bond path would, however, require an analysis of the various contributions to the hydrogen bond interaction not only from the donor and acceptor cores and hydrogen but also from the lone pairs. Here, we resort to a simpler method to determine how the lone pairs on the donor and acceptor atoms, as distinct from their cores, participate in the formation of hydrogen bonds and influence the location of the CP in the H···O region.

Taking the example of a typical hydrogen bond, say l(**II**) (Figure 2b), we see that one of its lone-pair lobes is inclined toward the hydrogen, the distance from its CP to hydrogen being shorter (1.43 Å) than the H···O distance (1.68 Å). The lone pair under consideration would certainly affect the H···O density. By considering the lone pairs distinctly (apart from the atomic cores of the D and A), we are able to obtain useful insights. We have paid attention to the location of the H···O CP with respect to a new interaction line (distinct from the atomic interaction line) connecting the hydrogen and the CP of the lone pair. Similar considerations involving the A and D atomic cores and the lone pairs (A_l and D_l) on the donor and acceptor oxygens give rise to a unique set of possibilities termed L_{i-j}, as depicted in Figure 6. In this Figure, the H···O CP is shown to lie on the interaction line L joining i and j objects, the latter corresponding to A, D, A_l, D_l, or H. In the linear hydrogen bond shown in Figure 6a, the H···O CP lies on the line joining the proton and the core of the acceptor. Here, i and j correspond to H and A, respectively, and we assign the symbol L_{H-A} to the description of the line. The l(**I**) bond belongs to this category. Besides L_{H-A}, we find another category involving the proton, L_{H-A_l} (Figure 6b), where the CP lies on the line joining a lone pair on the acceptor and the hydrogen. The b_{11} and b_{12} bonds of **IV** and l(**II**) belong to this category. Figure 6c−f depicts other possibilities. Thus, L_{D-A} (Figure 6c) implies that the CP lies on the line joining the donor and the acceptor.

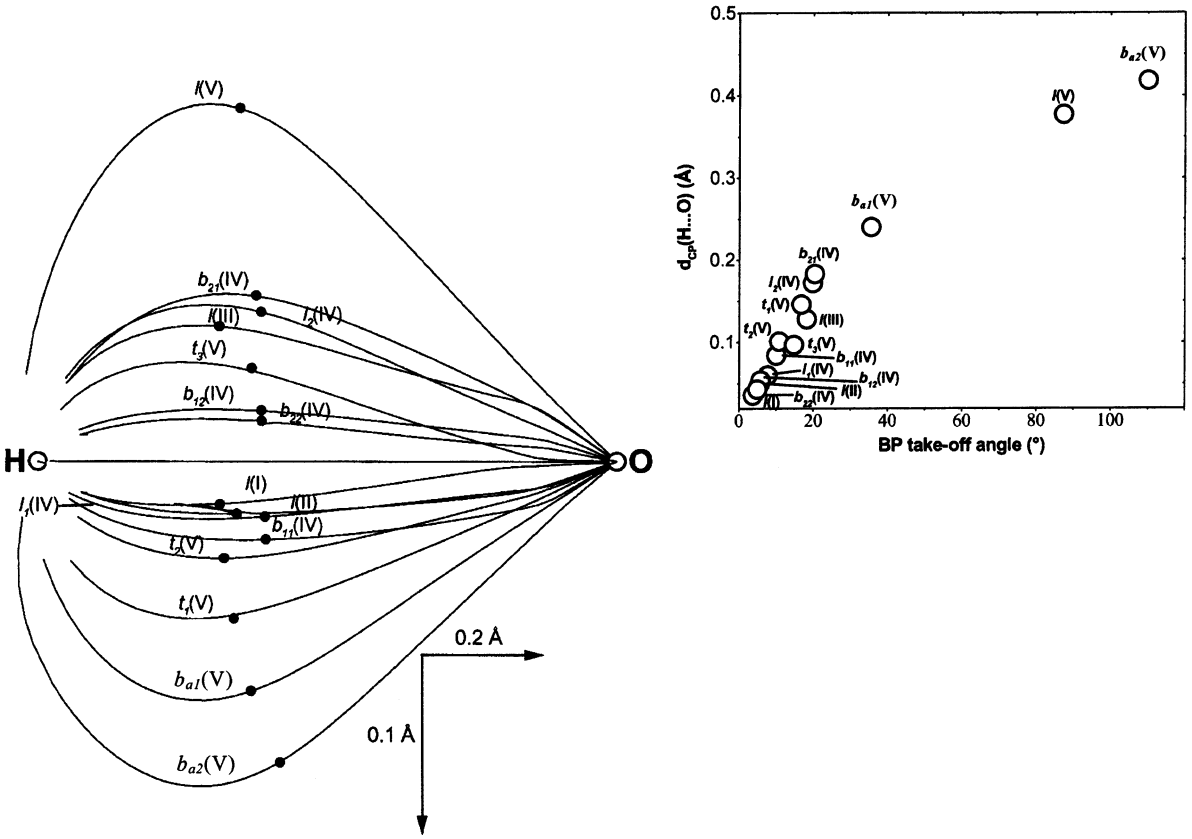

Figure 5. H···O bond paths normalized with respect to the H···O distance. The dark circles depict the H···O critical points. The type of hydrogen bond is shown above the bond path. The inset shows the variation of the d_{CP} values of the H···O bond with the corresponding bond path takeoff angle at the donor.

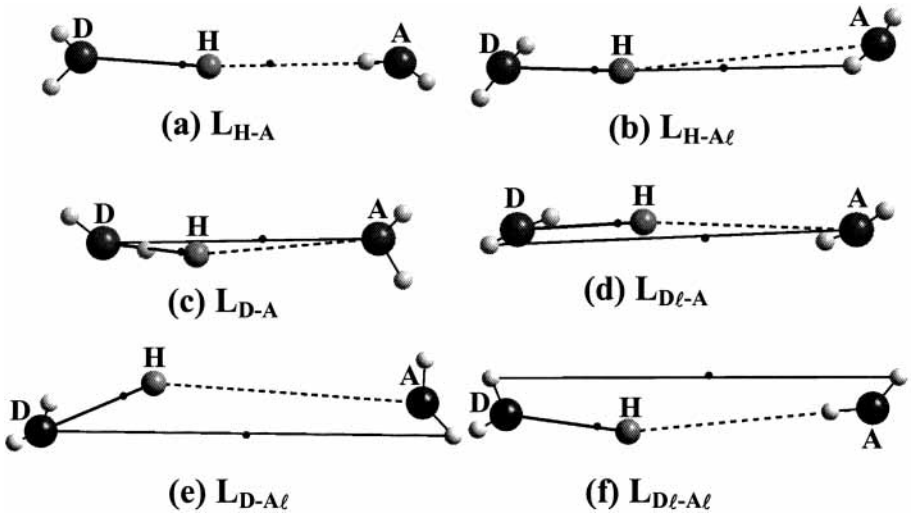

Figure 6. Schematic diagram showing connective relations. The open circles depict the hydrogen atoms. The O−H and H···O CPs are shown as tiny dark spheres. Six types of hydrogen bonds are depicted with different L_{i-j} relations, where L is the line joining i and j objects, the latter corresponding to the atomic cores (A and D), their lone pairs (A_l and D_l), or H. The L_{i-j} relation is established such that the H···O CP lies close to line L. (a) L_{H-A}, (b) L_{H-A_l}, (c) L_{D-A}, (d) L_{D_l-A}, (e) L_{D-A_l}, (f) $L_{D_l-A_l}$.

An example of this kind is t_3 in system **V**. L_{D_l-A} (Figure 6d) is the line joining a lone pair on the donor with the acceptor core. Bonds l of **III** and b_{a1} of **V** are examples of this category. Similarly, L_{D-A_l} (Figure 6e) stands for the line connecting the donor core with a lone pair on the acceptor, examples of this kind being b_{a2} and t_1 of **V**. The $L_{D_l-A_l}$ category (Figure 6f) where the CP lies in the line of sight of the lone pair on the donor and the lone pair on the acceptor finds many examples in the l_1, l_2, b_{21}, and b_{22} hydrogen bonds of **IV** as well as l and t_2 of **V**.

Let us consider in detail the simple case of the linear hydrogen bond l(**I**) shown in Figure 7a. Here, the O−H CP essentially lies on the internuclear axis (d_{CP}, 0.014 Å), and that in the H···O region with a d_{CP} value of 0.036 Å is well within that allowed for a bent bond. This hydrogen bond can be considered to belong to class L_{H-A}. The lone pairs on the donor are pointing in a direction opposite to that of the H···O bond with an angle of 94.7°, and those on the acceptor are more spread out with an angle of 145.6°. Figure 7b contains the linear bond, l(**III**). The

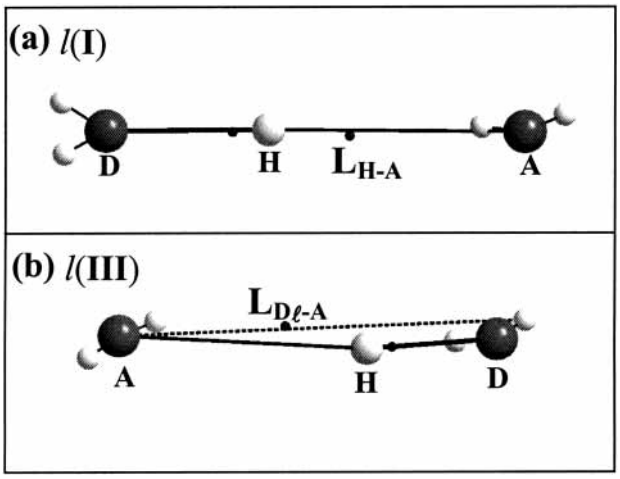

Figure 7. Connective relations in linear hydrogen bonds. The small gray spheres depict the lone pairs. The O−H and H···O CPs are shown as tiny dark spheres. (a) *l*(**I**) bond exhibiting relation L_{H-A}; (b) *l*(**III**) bond of class L_{D_l-A}.

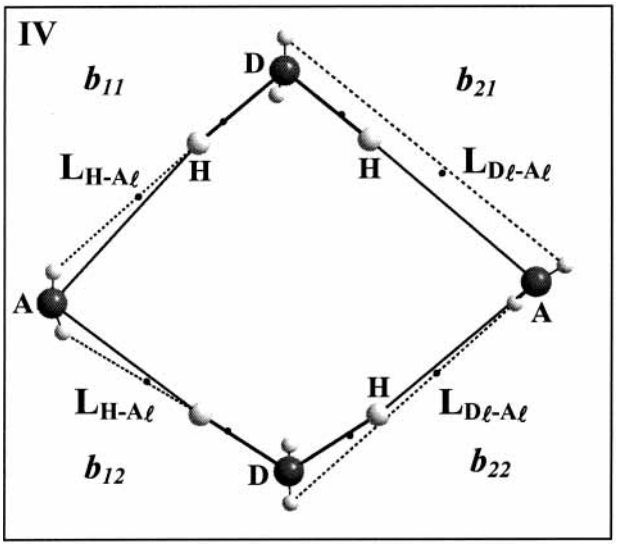

Figure 8. Connective relations in bifurcated hydrogen bonds in **IV**. The small gray spheres depict the lone pairs. The O−H and H···O CPs are shown as tiny dark spheres. Note that both of the lone pairs on the acceptor (A) are involved in bonding, but only one lone pair on each water donor (D) is engaged. The bond symbol and its class are shown alongside each bond.

O−H CP is on the internuclear line (d_{CP}, 0.006 Å), but the H···O CP is significantly away from the respective line with a d_{CP} of 0.128 Å. It is striking, however, that the H···O CP lies close to the line joining a lone pair on the donor and the acceptor core. Thus, the *l*(**III**) bond belongs to class L_{D_l-A}. It is convenient to define the perpendicular distance of the CP from line L as "the nearness parameter", d_L, that characterizes the different hydrogen bonds. The value of d_L for *l*(**III**) is 0.018 Å, which is remarkably smaller than its d_{CP} value (0.128 Å).

In Figure 8, we show the new connective relations in the two bifurcated bonds of **IV** where the same donor water molecules are shared by the two bonds. The b_{11} and b_{12} bonds of bifurcated system b_1 exhibit L_{H-A_l} relations engaging both of the lone pairs of the acceptor. The d_L values are similar (0.007 Å) and lower than the corresponding H···O d_{CP} values (Table 4). However, the b_{21} and b_{22} bonds of b_2 exhibit $L_{D_l-A_l}$ relations involving both of the lone pairs of the acceptor with d_L values of 0.042 and 0.014 Å, respectively. There seems to be some sort of cooperative effect in that the hydrogen bonds belonging to a bifurcated system tend to exhibit similar relations because of the suitable orientation of the acceptor lone pairs. The lone pair−core−lone pair (A_l −A−A_l) angle in both cases is 159.1°, which is also reflected in similar bifurcation angles (88.6 and 85.1°) of the hydrogen bonds. Whereas one lone pair from each donor water molecule is involved in establishing an L_{H-A_l} or $L_{D_l-A_l}$ relation, the other lone pair orients itself in a manner that minimizes the lone pair−lone pair repulsion. The corresponding φ_D angles for b_1 and b_2 pairs of bonds are 148.5 and 162.4°, respectively (Table 3).

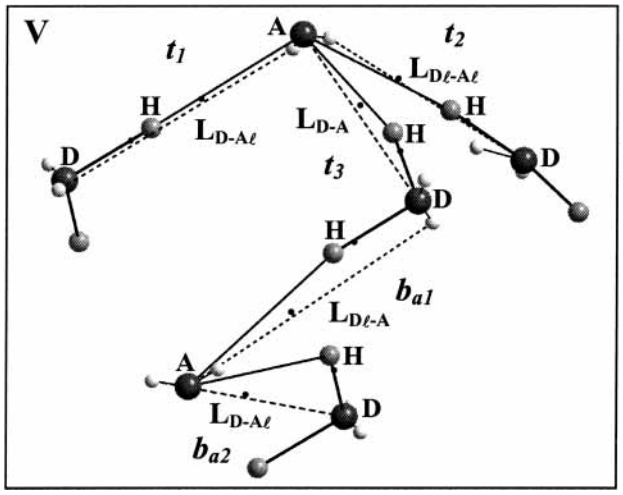

Figure 9. Connective relations in trifurcated and bifurcated hydrogen bonds in **V**. The small gray spheres depict the lone pairs. The O−H and H···O CPs are shown as tiny dark spheres. The bond symbol and its class are shown alongside each bond.

Cooperative effects are not found in bifurcated bond b_a of **V**, which is shown in Figure 9. Here, the two bonds belong to two different relations, perhaps because of the asymmetric nature of the bifurcation. The longer H···O bond (b_{a2}) follows an L_{D-A_l} relation, and the shorter bond (b_{a1}) obeys an L_{D_l-A} relation. The d_L values are small at 0.017 and 0.053 Å compared to d_{CP} values of 0.418 and 0.240 Å, respectively. The trifurcated bonds provide examples of L_{D-A}, L_{D-A_l}, and $L_{D_l-A_l}$ relations, where water molecules also act as common donors.

In Table 5, we list the various hydrogen bonds studied by us along with their descriptions and respective d_L values. Besides the examples discussed above, we have added some more examples to the list—three from a low-temperature form of adipic acid[27] (**VI**) and one from the γ polymorph of ethoxy cinnamic acid[25] (**VII**). The d_L values for the listed L_{i-j} relations are below 0.04 Å, and the corresponding d_{CP} were as high as 0.12 Å. From Tables 4 and 5, we notice that whenever the d_{CP} value is higher than permissible (say, up to 0.04 Å) a new connective relation (L_{i-j}) is generally obtained with the smallest possible d_L value. For example, the *l*(**V**) bond belonging to the $L_{D_l-A_l}$ class exhibits a d_L value of 0.043 Å compared to a d_{CP} value of 0.377 Å. However, one can obtain a whole spectrum of d_L values that are considerably larger by assuming that this bond belongs to the other classes depicted in Figure 6. Thus, the next-nearest d_L value for *l*(**V**) is 0.153 Å. Although most of the hydrogen bonds may permit a clear-cut assignment of the L_{i-j} type, it may prove difficult in certain situations. The b_{11} and b_{12} bonds of **IV** with the smallest d_L values (0.007 Å) in L_{H-A_l} have the next-nearest d_L values at 0.019 Å (L_{D-A_l}) and 0.047 Å ($L_{D_l-A_l}$) with average values of 0.143 and 0.135 Å, respectively. Because the d_L values in L_{H-A_l} are so low, the original assignments are still justifiable. Another example is the l_2(**IV**) bond where the d_L values from the $L_{D_l-A_l}$, L_{D-A_l}, and

TABLE 5: Classification of the Hydrogen Bonds on the Basis of the Critical Point Position with Their Respective Nearness Parameter[a]

system	type of H bond	class	$d_L \times 10^2$ (Å)
I	linear (l)	L_{H-A}	
II	linear (l)	L_{H-A_l}	3.3
III	linear (l)	L_{D_l-A}	1.8
IV	linear (l_1)	$L_{D_l-A_l}$	4.4
	linear (l_2)	$L_{D_l-A_l}$	7.0
	bifurcated (b_{11})	L_{H-A_l}	0.7
	bifurcated (b_{12})	L_{H-A_l}	0.7
	bifurcated (b_{21})	$L_{D_l-A_l}$	4.2
	bifurcated (b_{22})	$L_{D_l-A_l}$	1.4
V	linear (l)	$L_{D_l-A_l}$	4.3
	bifurcated (b_{a1})	L_{D_l-A}	5.3
	bifurcated (b_{a2})	L_{D-A_l}	1.7
	trifurcated (t_1)	L_{D-A_l}	3.0
	trifurcated (t_2)	$L_{D_l-A_l}$	3.6
	trifurcated (t_3)	L_{D-A}	8.5
VI	linear (l)	L_{D-A}	3.9
	linear (l)	L_{H-A}	
	linear (l)	L_{D-A}	3.7
VII	linear (l)	L_{D_l-A}	1.0

[a] For a description of class, see Figure 6 and the text. **VI**: low-temperature form of adipic acid; **VII**: γ form of ethoxy cinnamic acid. L_{i-j} stands for the class, where the H···O BCP lies close to the line joining i and j objects. D and A stand for the donor and the acceptor atom cores, and D_l and A_l, for the lone pairs on the donor and the acceptor atom cores, respectively. For L_{H-A}, $d_L = d_{CP}$.

L_{H-A_l} relations are similar (0.069, 0.073, and 0.070 Å, respectively), but all of them are considerably lower than the d_{CP} value (0.172 Å). Such situations reflect only the complex nature of interactions in the hydrogen-bonded system and may require further analysis. Nevertheless, the above discussion should suffice to demonstrate how on the basis of charge density analysis one is able to provide a better description of a hydrogen bond in terms of the location of the CP vis-à-vis the location of the lone pair of electrons on the donor and the acceptor atoms.

This study clearly brings out the unusual nature of the bond paths and the associated d_{CP} values in hydrogen bonds. In some sense, these situations are comparable to bent bonds observed in shared interactions, but the shape of the bond path as well as the magnitude of d_{CP} point to the more complex nature of the hydrogen bond interaction. This unusual behavior of the hydrogen bond has been examined here for the first time, taking examples from O−H···O bonds. Significantly, this work demonstrates how, using a simple rationale, apparently flexible unruly lone pairs on the donor and acceptor atoms can be linked to the hydrogen bond interaction in the vicinity, thereby providing insight into the observed diverse geometries. Clearly, the hydrogen bond interaction is more than a simple H···A interaction. Besides providing a useful classification, this study deepens our understanding of the cooperative effects in hydrogen bonds, as illustrated in the case of bifurcated hydrogen bonds.

Conclusions

We have employed the experimental charge density method to investigate several O−H···O hydrogen-bonded systems with a wide range of H···O distances (1.5−2.5 Å) and angles (130−176°) to obtain a more detailed understanding of the hydrogen bond. The examples include, besides simple linear bonds, symmetric and asymmetric bifurcated bonds as well as trifurcated bonds where two or three hydrogen bonds share a single acceptor atom. The total density and the Laplacian at the H···O critical point generally fall in the ranges of 0.07−0.4 eÅ^{-3} and 1.9−6.2 eÅ^{-5}, respectively, but the bond paths are often highly curved and displaced away from the H···O axis by as much as 0.4 Å (d_{CP} value) at the critical point. All such properties have been compiled in the present study. To explain the high d_{CP} values, the geometry of the lone pairs on the donor and the acceptor oxygen atoms has been specifically employed for the first time. The location of the critical point can be usefully related to a new interaction line, L_{i-j}, connecting i and j objects, representing the hydrogen (H) as well as the acceptor core (A), the donor core (D), and their lone pairs (A_l, D_l). This enables a classification of hydrogen bond interactions in terms of L_{H-A}, L_{H-A_l}, L_{D-A}, L_{D_l-A}, L_{D-A_l}, and $L_{D_l-A_l}$ relations. Furthermore, it is possible to define a nearness parameter, d_L, representing the perpendicular distance of the CP from line L. In general, the d_L values are much smaller than the corresponding d_{CP} values. The present study clearly shows how the charge density distribution (location of bond CP) in the hydrogen bond is related to the lone pairs as well as the cores of the donor and the acceptor atoms.

Supporting Information Available: Rigid-body model libration corrections for bond distances and the Hirshfeld rigid-bond test. Multipole populations. This material is available free of charge via the Internet at http://pubs.acs.org.

References and Notes

(1) (a) Koritsanszky, T. S.; Coppens, P. *Chem. Rev.* **2001**, *101*, 1583. (b) Kulkarni, G. U.; Gopalan, R. S.; Rao, C. N. R. *J. Mol. Struct.: THEOCHEM* **2000**, *500*, 339. (c) Coppens, P. *X-ray Charge Densities and Chemical Bonding*; Oxford Science Publishing: Oxford, U.K., 1997. (d) Tsierelson, V. G.; Ozerov, R. P. *Electron Density and Bonding in Crystals*; Institute of Physics Publishing: Bristol, U.K., 1996. (e) Jeffrey, G. A.; Piniella, J. F. *The Application of Charge Density Research to Chemistry and Drug Design*; Plenum Publishing: New York, 1991.

(2) (a) Dahaoui, S.; Pichon-Pesme, V.; Howard, J. A. K.; Lecomte, C. *J. Phys. Chem. A* **1999**, *103*, 6240. (b) Koritsanszky, T.; Flaig, R.; Zobel, D.; Krane, H.-G.; Morgenroth, W.; Luger, P. *Science* **1998**, *279*, 356.

(3) (a) Fkyerat, A.; Guelzim, A.; Baert, F.; Zyss, J.; Perigaud, A. *Phys. Rev. B* **1996**, *53*, 16236. (b) Hamzaoui, F.; Baert, F.; Zyss, J. *J. Mater. Chem.* **1996**, *6*, 1123. (c) Howard, S. T.; Hursthouse, M. B.; Lehmann, C. W.; Mallinson, P. R.; Frampton, C. S. *J. Chem. Phys.* **1992**, *97*, 5616.

(4) (a) Cole, J. M.; Goeta, A. E.; Howard, J. A. K.; McIntyre, G. J. *Acta Crystallogr., Sect. B* **2002**, *58*, 690. (b) Gopalan, R. S.; Kulkarni, G. U.; Rao, C. N. R. *New J. Chem.* **2001**, *25*, 1108. (c) Gopalan, R. S.; Kulkarni, G. U.; Rao, C. N. R. *ChemPhysChem* **2000**, *1*, 127.

(5) Madsen, G. K. H.; Krebs, F. C.; Lebech, B.; Larsen, F. K. *Chem.—Eur. J.* **2000**, *6*, 1797.

(6) (a) Cameron, T. S.; Borecks, B.; Kwiatkowski, W. *J. Am. Chem. Soc.* **1994**, *116*, 1211. (b) Bürgi, H.-B.; Capelli, S. C.; Goeta, A. E.; Howard, J. A. K.; Spackman, M. A.; Yufit, D. S. *Chem.—Eur. J.* **2002**, *8*, 3512.

(7) (a) Stewart, R. F. in ref 1e. (b) Fuhrmann, P.; Koritsanszky, T.; Luger, P. *Z. Kristallogr.* **1997**, *212*, 213.

(8) Destro, R.; Merati, F. *Acta Crystallogr., Sect. B* **1995**, *51*, 559.

(9) Irngartinger, H.; Strack, S. *J. Am. Chem. Soc.* **1998**, *120*, 5818.

(10) Ranganathan, A.; Kulkarni, G. U. *J. Phys. Chem. A* **2002**, *106*, 7813.

(11) (a) Macchi, P.; Iversen, B. B.; Sironi, A.; Chakoumakos, B. C.; Larsen, F. K. *Angew. Chem., Int. Ed.* **2000**, *39*, 2719. (b) Kulkarni, G. U.; Kumaradhas, P.; Rao, C. N. R. *Chem. Mater.* **1998**, *10*, 3498. (c) Madsen, G. K. H.; Iversen, B. B.; Larsen, F. K.; Kapon, M.; Reisner, G. M.; Herbstein, F. H. *J. Am. Chem. Soc.* **1998**, *120*, 10040. (d) Madsen, D.; Flensburg, C.; Larsen, S. *J. Phys. Chem. A* **1998**, *102*, 2177. (e) Hermansson, K.; Tellgren, R. *Acta Crystallogr., Sect. B* **1989**, *45*, 252. (f) Krijn, M. P. C. M.; Feil, D. *J. Chem. Phys.* **1988**, *89*, 4199. (g) Blessing, R. H. *Acta Crystallogr., Sect. B* **1988**, *44*, 334. (h) Gajhede, M.; Larsen, S.; Rettrup, S. *Acta Crystallogr., Sect. B* **1986**, *42*, 545. (i) Hermansson, K.; Thomas, J. O. *Acta Crystallogr., Sect. B* **1982**, *38*, 2555.

(12) (a) Rodrigues, B. L.; Tellgren, R.; Fernandes, N. G. *Acta Crystallogr., Sect. B* **2001**, *57*, 353. (b) Overgaard, J.; Schiott, B.; Larsen, F. K.; Iversen, B. B. *Chem.—Eur. J.* **2001**, *7*, 3756. (c) Ellena, J.; Goeta, A. E.; Howard, J. A. K.; Punte, G. *J. Phys. Chem. A* **2001**, *105*, 8696. (d) Stevens, E. D.; Rys, J.; Coppens, P. *J. Am. Chem. Soc.* **1978**, *100*, 2324. (e) Coppens, P.; Vos, A. *Acta Crystallogr., Sect. B* **1971**, *27*, 146. (f) Verschoor, G. C.; Keulen, E. *Acta Crystallogr., Sect. B* **1971**, *27*, 134.

(13) (a) Mallinson, P. R.; Woźniak, K.; Wilson, C. C.; McCormack, K. L.; Yufit, D. S. *J. Am. Chem. Soc.* **1999**, *121*, 4640. (b) Mallinson, P. R.; Woźniak, K.; Smith, G. T.; McCormack, K. L. *J. Am. Chem. Soc.* **1997**, *119*, 11502.

(14) (a) Gatti, C.; May, E.; Destro, R.; Cargnoni, F. *J. Phys. Chem. A* **2002**, *106*, 2707. (b) Macchi, P.; Schultz, A. J.; Larsen, F. K.; Iversen, B. B. *J. Phys. Chem. A* **2001**, *105*, 9231. (c) May, E.; Destro, R.; Gatti, C. *J. Am. Chem. Soc.* **2001**, *123*, 12248.

(15) (a) Bakshi, P. K.; Cameron, T. S.; Knop, O. *Can. J. Chem.* **1996**, *74*, 201. (b) Bianchi, R.; Gatti, C.; Adovasio, V.; Nardelli, M. *Acta Crystallogr., Sect. B* **1996**, *52*, 471. (c) Knop, O.; Cameron, T. S.; Bakshi, P. K.; Kwiatkowski, W.; Choi, S. C.; Adhikesavalu, D. *Can. J. Chem.* **1993**, *71*, 1495.

(16) Cameron, T. S.; Knop, O.; Kwiatkowski, W.; Robertson, K. N. *ACA Annual Meeting Abstracts*, St. Louis, MO, 1997.

(17) (a) Klooster, W. T.; Swaminathan, S.; Nanni, R.; Craven, B. M. *Acta Crystallogr., Sect. B* **1992**, *48*, 217. (b) Tonogaki, M.; Kawata, T.; Ohba, S. *Acta Crystallogr., Sect. B* **1993**, *49*, 1031. (c) Puig-Molina, A.; Alvarez-Larena, A.; Piniella, J. F.; Howard, S. T.; Baert, F. *Struct. Chem.* **1998**, *9*, 395. (d) Abramov, Y. A.; Brammer, L.; Klooster, W. T.; Bullock, R. M. *Inorg. Chem.* **1998**, *37*, 6317. (e) Dahaoui, S.; Jelsch, C.; Howard, J. A. K.; Lecomte, C. *Acta Crystallogr., Sect. B* **1999**, *55*, 226. (f) Gopalan, R. S.; Kumaradhas, P.; Kulkarni, G. U.; Rao, C. N. R. *J. Mol. Struct.* **2000**, *521*, 97. (g) Gopalan, R. S.; Kulkarni, G. U. *Proc. - Indian Acad. Sci., Chem. Sci.* **2001**, *113*, 307. (h) Coppens, P.; Abramov, Yu.; Carducci, M.; Korjov, B.; Novozhilova, I.; Alhambra, C.; Pressprich, M. R. *J. Am. Chem. Soc.* **1999**, *121*, 2585.

(18) On the other hand, there are a large number of studies that deal with trends in the structural parameters of the hydrogen bond. See (a) Jeffrey, G. A. *An Introduction to Hydrogen Bonding*; Oxford University Press: New York, 1997. (b) Jeffrey, G. A.; Saenger, W. *Hydrogen Bonding in Biological Structures*; Springer-Verlag: Berlin, 1991. (c) Desiraju, G. R. *Angew. Chem., Int. Ed. Engl.* **1995**, *34*, 2311. (d) Desiraju, G. R.; Steiner, T. *The Weak Hydrogen Bond*; Oxford University Press: Oxford, U.K., 1999. Besides, there are studies that relate the hydrogen bond to the lone-pair geometry based on crystallographic analysis, intuition, and theory. See (e) Hay, B. P.; Dixon, D. A.; Bryan, J. C.; Moyer, B. A. *J. Am. Chem. Soc.* **2002**, *124*, 182. (f) Steiner, T. *Chem. Commun.* **1997**, 727. (g) Platts, J. A.; Howard, S. T.; Bracke, B. R. F. *J. Am. Chem. Soc.* **1996**, *118*, 2726. (h) Legon, A. C.; Millen, D. J. *Acc. Chem. Res.* **1987**, *20*, 39. (i) Murray-Rust, P.; Glusker, J. P. *J. Am. Chem. Soc.* **1984**, *106*, 1018. (j) Taylor, R.; Kennard, O. *Acc. Chem. Res.* **1984**, *17*, 320. (k) Millen, D. J. *Croat. Chem. Acta* **1982**, *55*, 133. (l) Mitra, J.; Ramakrishnan, C. *Int. J. Pept. Protein Res.* **1977**, *9*, 27. (m) Kroon, J.; Kanters, J. A.; van Duijneveldt-van de Rijdt, J. G. C. M.; Vliegenhardt, J. *J. Mol. Struct.* **1975**, *24*, 109. (n) Ramakrishnan, C.; Prasad, N. *Int. J. Protein Res.* **1971**, *3*, 209. (o) Donohue, J. In *Strutural Chemistry and Molecular Biology*; Rich, A., Davidson, N., Eds.; W. H. Freeman: San Francisco, CA, 1968; p 443.

(19) Espinosa, E.; Souhassou, M.; Lachekar, H.; Lecomte, C. *Acta Crystallogr., Sect. B* **1999**, *55*, 563.

(20) (a) Espinosa, E.; Molins, E.; Lecomte, C. *Chem. Phys. Lett.* **1998**, *285*, 170. (b) Spackman, M. A. *Chem. Phys. Lett.* **1999**, *301*, 425.

(21) Espinosa, E.; Lecomte, C.; Molins, E. *Chem. Phys. Lett.* **1999**, *300*, 745.

(22) Woźniak, K.; Mallinson, P. R.; Wilson, C. C.; Hovestreydt, E.; Grech, E. *J. Phys. Chem. A* **2002**, *106*, 6897.

(23) Lin, K.-J.; Cheng, M.-C.; Wang, Y. *J. Phys. Chem.* **1994**, *98*, 11685.

(24) Several authors have carried out systematic studies of the relationship of the electron density parameters and the hydrogen bond geometry. See, for example, (a) Knop, O.; Rankin, K. N.; Boyd, R. J. *J. Phys. Chem. A* **2003**, *107*, 272. (b) Espinosa, E.; Alkorta, I.; Elguero, J.; Molins, E. *J. Chem. Phys.* **2002**, *117*, 5529. (c) Galvez, O.; Gomez, P. C.; Pacios, L. F. *J. Chem. Phys.* **2001**, *115*, 11166. (d) Knop, O.; Rankin, K. N.; Boyd, R. J. *J. Phys. Chem. A* **2001**, *105*, 6552.

(25) Gopalan, R. S.; Kulkarni, G. U.; Subramanian, E.; Renganayaki, S. *J. Mol. Struct.* **2000**, *524*, 169.

(26) Vaidhyanathan, R.; Natarajan, S.; Rao, C. N. R. *J. Mol. Struct.* **2001**, *608*, 123.

(27) Gopalan, R. S.; Kumaradhas, P.; Kulkarni, G. U. *J. Solid State Chem.* **1999**, *148*, 129.

(28) Allen, F. H.; Kennard, O.; Watson, D. G.; Brammer, L.; Orpen, A. G.; Taylor, R. *J. Chem. Soc., Perkin Trans. 2* **1987**, S1.

(29) Spek, A. L. *PLATON, Molecular Geometry Program*; University of Utrecht: Utrecht, The Netherlands, 1995.

(30) Koritsanszky, T.; Howard, S. T.; Richter, T.; Mallinson, P. R.; Su, Z.; Hansen, N. K. *XD, A Computer Program Package for Multipole Refinement and Analysis of Charge Densities from Diffraction Data*; Cardiff, Glasgow, Buffalo, Nancy, Berlin, 1995.

(31) Hirshfeld, F. L. *Acta Crystallogr., Sect. A* **1976**, *32*, 239.

(32) Bader, R. F. W. *Atoms in Molecules*: *A Quantum Theory*; Clarendon Press: Oxford, U.K., 1990.

(33) Cremer, D.; Kraka, E. *Croat. Chem. Acta* **1984**, *57*, 1259.

(34) Popelier, P. *Atoms in Molecules*: *An Introduction*; Prentice Hall: New York, 2000; Chapter 5.

(35) (a) Page 47 of ref 30. (b) Howard, S. T.; Hursthouse, M. B.; Lehmann, C. W. *Acta Crystallogr., Sect. B* **1995**, *51*, 328. (c) Hermansson, K.; Tellgren, R. *Acta Crystallogr., Sect. B* **1989**, *45*, 252.

(36) (a) Ciechanowicz-Rutkowska, M.; Kiec-Kononowicz, K.; Howard, S. T.; Lieberman, H.; Hursthouse, M. B. *Acta Crystallogr., Sect. B* **1994**, *50*, 86. (b) Smith, G. T.; Mallinson, P. R.; Frampton, C. S.; Farrugia, L. J.; Peacock, R. D.; Howard, J. A. K. *J. Am. Chem. Soc.* **1997**, *119*, 5028. (c) Dittrich, B.; Flaig, R.; Koritsanszky, T.; Krane, H.-G.; Morgenroth, W.; Luger, P. *Chem.—Eur. J.* **2000**, *6*, 2582. (d) Macchi, P.; Iversen, B. B.; Sironi, A.; Chakoumakos, B. C.; Larsen, F. K. *Angew. Chem., Int. Ed.* **2000**, *39*, 2719. We found it convenient and straightforward to deal with deformation density instead of the Laplacian.

(37) Many other systems with such bifurcated hydrogen bonds are known. See, for example, (a) Berkovitch-Yellin, Z.; Leiserowitz, L. *Acta Crystallogr., Sect. B* **1984**, *40*, 159. (b) Marsden, C. J.; Smith, B. J.; Pople, J. A.; Schaefer, H. F.; Radon, L. *J. Chem. Phys.* **1991**, *95*, 1825. (c) Mó, O.; Yáñez, M.; Elguero, J. *J. Chem. Phys.* **1992**, *97*, 6628. (d) Louit, G.; Hocquet, A.; Ghomi, M.; Meyer, M.; Sühnel, J. *PhysChemComm* **2002**, *5*, 94. Many examples of bifurcated hydrogen bonds are known where the hydrogen atom from a single donor group is bonded to two acceptor atoms. Such a configuration is also termed a three-centered interaction. See (e) Albrecht, G.; Corey, R. B. *J. Am. Chem. Soc.* **1939**, *61*, 1087. (f) Marsh, R. E. *Acta Crystallogr.* **1958**, *11*, 654. (g) Jönsson, P. G.; Kvick, A. *Acta Crystallogr., Sect. B* **1972**, *28*, 1827. (h) Jeffrey, G. A.; Mitra, J. *J. Am. Chem. Soc.* **1984**, *106*, 5546. (i) Rozas, I.; Alkorta, I.; Elguero, J. *J. Phys. Chem. A* **1998**, *102*, 9925. (j) Goutev, N.; Matsuura, H. *J. Phys. Chem. A* **2001**, *105*, 4741.

(38) The hydrogen bonds chosen in the present study satisfy the criteria of Koch and Popelier (Koch, U.; Popelier, P. L. A. *J. Chem. Phys.* **1995**, *99*, 9747), one of them being the presence of a bond path for the H···O bond carrying a critical point with finite electron density (>0.02 eÅ^{-3}) and the Laplacian (>1 eÅ^{-5}).

(39) Cremer, D.; Kraka, E. *J. Am. Chem. Soc.* **1985**, *107*, 3800.